

Supplementary Information to:

Heberling et al., Electrolyte layering at the calcite(104)-water interface indicated by Rb^+ - and Se(VI) K-edge resonant interface diffraction

Resonant anomalous dispersion terms for Rb^+ and Se(VI)

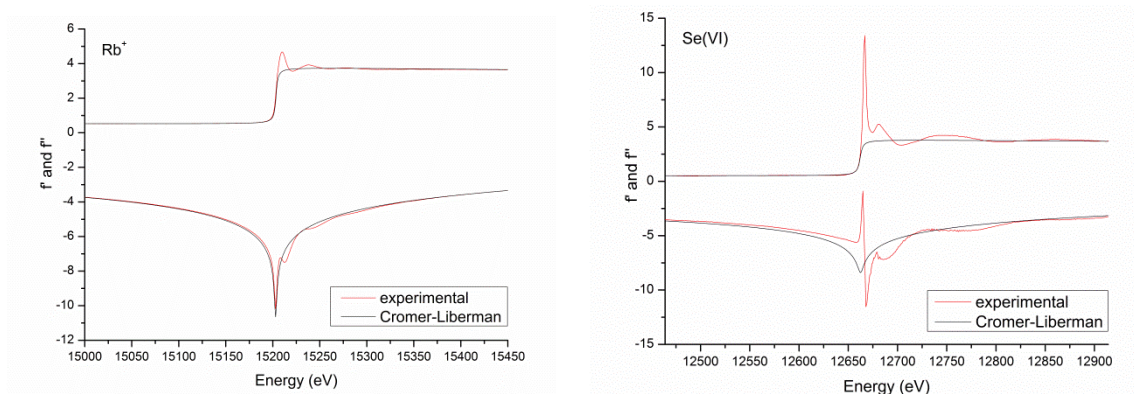


Fig. S1: Experimentally determined and Cromer-Lieberman calculated resonant anomalous dispersion terms $f'(E)$ and $f''(E)$ for Rb^+ and Se(VI) . Cromer-Lieberman curves are shifted in energy to match the experimental absorption edges. It is interesting to note the effect of the extreme white line of Se(VI) on the experimental $f'(E)$ function. In contrast, the experimental dispersion terms of Rb^+ only show some minor fine structure oscillations around the Cromer-Lieberman curves.

Spatial resolution for resonant data analysis and direct space volume probed by resonant data

Each resonant scan corresponds to one Fourier component describing the electron density distribution related to the distribution of the resonant element at the interface. Accordingly, the spatial resolution of the measurements, Δz , is determined by the resonant scan measured at maximum momentum transfer, $|\mathbf{Q}_{\max}|$, such that $\Delta z = 1/|\mathbf{Q}_{\max}|$ (reciprocal space vectors used here are defined in a way that $\mathbf{h} \cdot \mathbf{h}^* = 1$). Measurements at calcite (104) up to $L \sim 4$, using a unit cell that includes two (104) layers in the z direction, corresponds to a resolution of $\Delta z \approx 1.5 \text{ \AA}$. On the other hand, data are sensitive to the area around the origin determined by step sizes, ΔH_{\min} , ΔK_{\min} , and ΔL_{\min} , at which resonant scans are recorded. For Rb^+ , the data recorded are sensitive to a box of 0.5 unit cells in x , 1 unit cell in y , and 5 unit cells in z , or ca. $4 \text{ \AA} \times 5 \text{ \AA} \times 30 \text{ \AA}$ (15 \AA above and below the surface) around the origin. The glide plain symmetry along the x -axis of the unit cell allows to extrapolate results from one half of the unit cell to the second half of the unit cell along the x -direction.

Details on the layered electrolyte model

The layered electrolyte model can be imagined as a series of Gaussians along the surface normal direction appearing at a constant distance, d . The width of the Gaussians, σ^2 , is in the following noted as

U for reasons of consistency with the Debye-Waller parameters used for the other atoms in the interface model. As for the layered water model, U is assumed to increase constantly about U_{bar} with each consecutive layer starting from the width of the first Gaussian, U_0 , such that the width of the n^{th} Gaussian is given by $U_n = U_0 + n U_{bar}$. Additionally, the occupancy, ϕ , of each layer is allowed to vary exponentially with distance from the surface, such that the occupancy of the n^{th} layer is given by, $\phi_n = \phi_0 \exp(-k d n)$, where k is the decay-constant of the layer occupancy. This is meant to resemble the concentration decrease with distance from the surface as, e.g., expected for Gouy-Chapman behavior in the diffuse part of the electric double layer. The exponential function is certainly a crude adaption to the concentration profile expected according to Gouy-Chapman theory, especially because it approaches zero for infinite distance from the surface for $k > 0$ (and infinite for $k < 0$) and not a constant bulk concentration. However, within the region resonant data are sensitive to, up to 10 Å or 15 Å above the surface in the present case (some 10 Ångstroems may be relevant for other systems and measurement parameters), concentration distributions produced by this simple function are very similar to those expected according to Gouy-Chapman theory for low diffuse layer potentials. An exemplary comparison between the layered electrolyte model and a Gouy-Chapman model (using the Poisson Boltzmann equation for mixed electrolytes) is shown in the next section of this supplementary information file (Figures S2 and S3). Calculation of structure factors according to the simple exponential function is already rather challenging. Therefore, more complex models were not attempted. As will be discussed below, concentration profiles within the first 10 Å to 15 Å above the surface derived from the resonant interface diffraction data in this study appeared to be different from any expected diffuse layer behaviour.

The described model leads to a contribution of the layered resonant element structure, $F_{lay_res_el}(\mathbf{Q})$, to the total structure factor, which is given by the infinite geometric series:

$$F_{lay_res_el}(\vec{Q}) = \phi_0 \exp(-2\pi^2 Q^2 U_0 + i 2\pi \vec{Q} z_0) \sum_{n=0}^{\infty} \exp[n(-2\pi^2 Q^2 U_{bar} - kd + i 2\pi \vec{Q} d)].$$

This leads to the expression:

$$F_{lay_res_el}(\vec{Q}) = \phi_0 \exp(-2\pi^2 Q^2 U_0 + i 2\pi \vec{Q} z_0) / [1 - \exp(-2\pi^2 Q^2 U_{bar} - kd + i 2\pi \vec{Q} d)].$$

Note that differences between this expression and the one given in Fenter and Sturchio (2004)¹ (beyond ϕ_0 and the $-k d$ term), originate from a different definition of reciprocal space vectors, as described above, and from the use of U tensors instead of σ^2 to describe thermal vibrations. To calculate the influence of this model on the resonant structure factors, $F_{lay_res_el}(\mathbf{Q})$ needs to be multiplied by the anomalous dispersion terms of the resonant element, $[f'(E) + i f''(E)]$. To calculate the influence of this model on the non-resonant structure factors, $F_{lay_res_el}(\mathbf{Q})$ needs to be multiplied by the non-resonant atom form factor, $f(\mathbf{Q})$, of the resonant element.

Comparison between the layered electrolyte model and the Poisson-Boltzmann solution for mixed electrolytes at low diffuse layer potential

In the resonant interface diffraction experiment in the presence of RbCl, the solution contains 10 mmol/L RbCl. Due to equilibration with calcite pH is 8.3 the Ca^{2+} concentration is 0.6 mmol/L and the HCO_3^- concentration is 1.2 mmol/L. Correspondingly, we initially expected the diffuse layer potential to be slightly positive (~8 mV), which might correspond to a zetapotential of ~ 5mV and would be in line with previous experiments. The expected potential- and concentration gradients within the diffuse layer are

shown in Figure S2. Concentrations at the onset of the diffuse layer are expected to change only slightly compared to concentrations in bulk water.

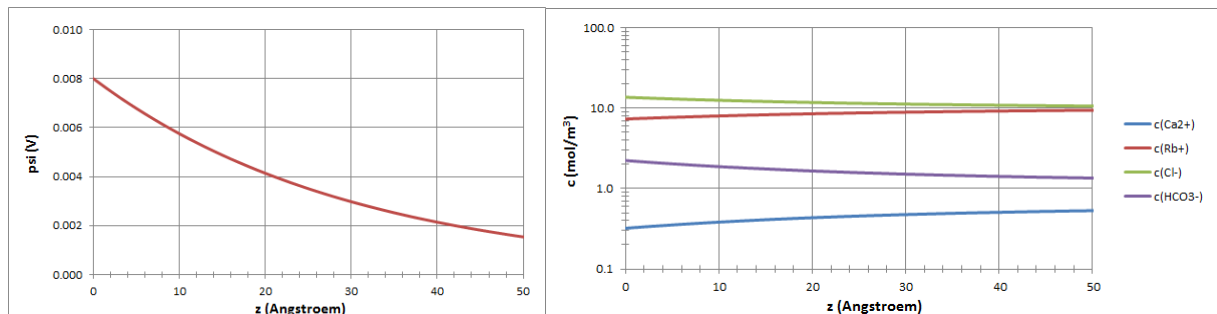


Fig. S2: Diffuse layer potential- (left) and concentration gradients (right) according to the Poisson-Boltzmann equation for mixed electrolytes as commonly used in the Gouy-Chapman model.

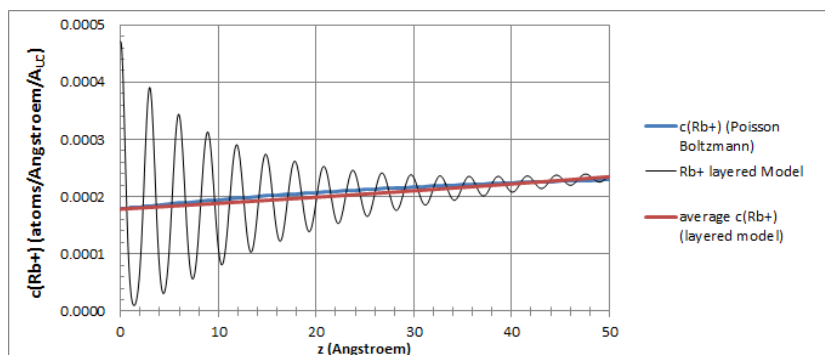


Fig. S3: Comparison between Rb^+ concentration gradients according to Poisson-Boltzmann, the layered electrolyte model, and the average over the layered electrolyte model. For comparison to occupancy values, concentrations are given in atoms per \AA , normalized to the area of a surface unit cell (A_{UC}). In average, the layered model and the Poisson-Boltzmann model match almost perfectly. This holds only as long as the diffuse layer potential is small (± 20 mV).

It is shown in Figure S3 that at these conditions the average over a layered electrolyte structure with exponentially increasing layer occupancy (red line in Figure S3) matches almost exactly with the expected concentration gradient according to the Poisson-Boltzmann model over some nanometers above the surface (blue line in Figure S3). This holds only as long as the diffuse layer potential is small (± 20 mV). At higher diffuse layer potentials the exponential model fails to get the curvature of the concentration gradient right. The good match between the two curves is meant to verify the use of the simple exponential occupancy model in the analysis of resonant interface diffraction data indicating a layering of the electrolyte.

However, as laid out in the main manuscript, the layer occupancy in the electrolyte layers according to resonant data analysis in this study is much higher than expected and does not indicate a concentration gradient which may be brought into agreement with the Poisson-Boltzmann equation.

Estimation of uncertainties of variables adjusted to fit the resonant data

The estimation of uncertainties applied in the python interface structure refinement code follows closely the approach used in the USGS software UCODE². This approach works nicely for CTR data and is robust. However, for resonant data there are some issues, which so far prevent realistic uncertainty calculation. For resonant data, the number of data points is large compared to the number of adjusted parameters. The number of data points affects the calculation of the uncertainty similarly as in the normalization of χ^2 (see main manuscript for details). Calculated uncertainties are therefore extremely low, e.g. in the order of 0.001% for the three parameters from the 1Rb model: occupancy: 0.21 Rb⁺ ions, z-position: 2.61 Å above the surface, distribution width $U_{33} = 1.56 \text{ Å}^2$. Many of the resonant data points are, however, mainly used to determine the linear background associated with the energy scan. As the structure dependent part of each scan is basically described by two parameters, A_R and P_R , we may reduce the number of data points from the number of measured points to two independent data points in each resonant scan. This partly fixes the problem; for example, uncertainties for the above mentioned parameters increase from ~0.001% to ~0.1%. Nevertheless, there are systematic errors, which have a more pronounced influence on the parameters than reflected by statistical uncertainty calculations. For example, knowledge of the thickness of the water film above the surface is required to calculate an absorption correction necessary to separate the resonant diffraction signal from the effect of x-ray absorption as the beam passes through the solution film. However, solution film thickness, usually in the order of 1 µm, is not known precisely. If the film thickness is varied between 0.1 µm and 10 µm, the absorption correction is calculated according to each thickness, and the 1Rb model parameters are optimized, we find that the height of Rb⁺ above the surface varies within $\pm 0.02 \text{ Å}$, the occupancy varies about ± 0.02 , and U_{33} varies about $\pm 0.1 \text{ Å}^2$. These error estimates seem much more realistic than the calculated fit uncertainties. For any parameters refined on resonant data it was therefore decided, not report the calculated uncertainties. Instead, only as many digits as considered significant based on systematic error propagation are listed.

Effect of a layered structure on the resonant amplitude, A_R

The thick black lines in Figure S4 correspond to a single inner-sphere adsorbed Rb⁺-species 1.21 Å above the surface with a surface coverage of 0.2 ML. In reciprocal space this corresponds to a monotonically decreasing trend in A_R . For $L = 0$, A_R is equal to the total surface coverage (0.2). The slope of the curve is determined by the distance of the Rb⁺-species from the surface and the thermal vibration parameter. If we add a second Rb⁺-species at 2.42 Å above the surface with equal surface coverage and thermal vibration, we obtain the red curves in Figure S4. Total surface coverage is now 0.4 ML. The L-position of the dip between the two maxima (L_d) in the A_R curve is related to the vertical distance, dz , between the two Rb⁺-species, such that $L_d = 1/(2dz) = 2.5$, where dz would be in fractional coordinates and $dz \cdot |c| = 1.21 \text{ Å}$. The important thing to note here is that the second maximum of the A_R curve is lower than the first. This decrease in the maxima of A_R versus L is typical for simple structures including two or three interfacial species. The only means to break this trend would be the presence of several species at a common vertical distance above the surface, i.e. a layered structure. For example, the green curves in Figure S4 correspond to a fictive structure of four equidistant Rb⁺ species. For this structure a peak starts

to appear in reciprocal space around $L = 1/dz = 5$. Projecting this further to the extreme case of an infinite equidistant structure in real space, produces a CTR profile in the A_R curve. This is illustrated with the violet curve in Figure S4, which is calculated using the equation of a semi-infinite layered structure presented above, with $\phi_0 = 0.2$, $K = 0$, $z_0 = 0.2$ ($= 1.21 \text{ \AA}$), $dz = 0.2$ ($= 1.21 \text{ \AA}$), and $U_{\text{bar}} = 0 \text{ \AA}^2$. This is of course unrealistic for a structure in aqueous solution. If $U_{\text{bar}} > 0 \text{ \AA}^2$ is used, the distribution width increases with each consecutive layer (orange curves in Figure S4), and the structure becomes equivalent to a layered bulk water profile. The peak in the A_R curve at $L = 5$ using $U_{\text{bar}} = 0.02 \text{ \AA}^2$ is still evident but decreases dramatically compared to the curve for $U_{\text{bar}} = 0 \text{ \AA}^2$. Similarly, using $K > 0$ causes a decrease in this peak (magenta curves in Figure S4). The effect of K and U_{bar} on A_R is similar, but differs in the influence of the parameters on the peak shape. Therefore, the correlation between K and U_{bar} is weak.

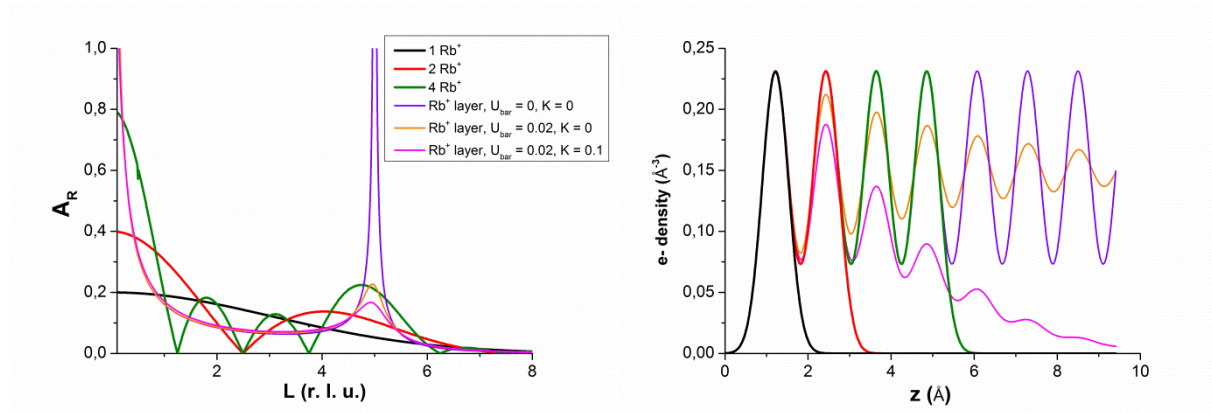


Fig. S4: Resonant amplitude, A_R , along the specular CTR as a function of specular momentum transfer (left) for various exemplary scenarios of Rb^+ distribution above the calcite(104) surface (right). (see text for details)

References

1. P. Fenter and N. C. Sturchio, *Progress in Surface Science*, 2004, **77**, 171-258.
2. E. P. Poeter and M. C. Hill, *Documentation of UCODE, a computer code for universal inverse modeling*, US Geological Survey, 1998.